International Journal of Wireless Information Networks, Vol. 4, No. 2, 1997

Wideband Propagation Measurements and Modeling in Indoor Environment

N. Papadakis,[1,2] A. Hatziefremidis,[1] A. Tserolas,[1] and P. Constantinou[1]

This paper presents the results of wideband measurements of an indoor wireless radio channel at 1.8 GHz. Propagation measurements were carried out in an indoor environment at the Technical University of Athens with a network analyzer. From the measured impulse response (IR) profiles collected, mean excess delay τ_m and root mean square of delay spread τ_{rms} have been estimated. Statistical analysis of delay spread and amplitude fading has been performed. Comparison with simulation results extracted from SIRCIM Simulator package has also been made.

KEY WORDS: Indoor radio propagation; wideband; delay spread.

1. INTRODUCTION

The strong growth of personal communication systems (PCS) and high-bit-rate wireless data networks has led to an increase of interest in wideband radio propagation characteristics within buildings. Detailed and accurate knowledge of radio propagation inside buildings is of great importance for the successful design of indoor wireless communications systems.

In an indoor radio environment where both transmitter and receiver are located in the same room, electromagnetic energy may travel directly from transmitter to receiver, but also via reflections from walls, ceiling, floor, and objects within the room.

The indoor radio channel is characterized by the complex impulse response function suggested by Turin [1], which is given by

$$h(t) = \sum \beta_n e^{-j\theta_n} \delta(t - \tau_n) \tag{1}$$

where β_n is the nth received normalized pulse (on the amplitude of the transmitted pulse) and τ_n and θ_n are the excess delay and phase for the nth ray, respectively.

With no movement of individuals during the measurements process, the time variation of the channel can be considered as static, although measurements during the motion of people will provide a full characterization of the indoor radio channel. Characterization of impulse response profile is based on rms delay spread, given by

$$\tau_{\text{rms}} = \left[\frac{\int_{-\infty}^{+\infty} (t - \tau_n)^2 |h(t)|^2 \, dt}{\int_{-\infty}^{+\infty} |h(t)|^2 \, dt} \right]^{1/2} \tag{2}$$

where τ_m is the mean excess delay defined as

$$\tau_m = \frac{\int_{-\infty}^{+\infty} t |h(t)|^2 \, dt}{\int_{-\infty}^{+\infty} |h(t)|^2 \, dt} \tag{3}$$

The rms delay spread computed from time-averaged

[1]Electrical and Computer Engineering Department, Electroscience Division, Mobile Communication Laboratory, National Technical University of Athens, 157 80 Zografou Athens, Greece.

[2]Correspondence should be directed to N. Papadakis, Electrical and Computer Engineering Department, Electroscience Division, Mobile CommunicationLaboratory, National Technical University of Athens, 9 Heroon Polytechniou 157 80 Zografou Athens, Greece; e-mail: npap@tinos.mobile.ece.ntua.gr.

1068-9605/97/0400-0101$12.50/0

impulse responses (IR) gives an indication of ISI and BER for different symbol rates and modulation schemes. More specifically, recent analysis and simulation tests have shown that with no diversity or equalization, maximum rate of data transmission in an indoor environment is a few percent of $1/\tau_{\text{rms}}$ [8]. As a result, it is necessary to describe the indoor multipath channel by correct τ_{rms} values. This paper is organized as follows: Section 2 describes the measurement environment, Section 3 describes the measurement apparatus and the experimental procedure, and Section 4 presents the data analysis, the results of fading statistics, and simulation tests using SIRCIM software [5]. Conclusion are given in Section 5.

2. MEASUREMENT ENVIRONMENT

Extensive multipath propagation measurements were carried out. The purpose of these measurements was full characterization of the propagation media, different in the environment compared to other reports, based on elaborate analysis and modeling of the impulse response data. Measurements have been conducted with and without motion of people and for LOS and NLOS cases. This paper describes experiments performed within a building at 1.8 GHz using a frequency domain measurement system incorporating a vector network analyzer. The measurements were conducted on the fourth floor of the Engineering Building at the National Technical University of Athens. The indoor radio environment as well as some of the examined measurement locations are shown in Fig. 1, and includes Room I, Room II, and the corridor. Measurements in Room I included locations A, B, C, D, and E with the receiving antenna remaining *static*, as well as location F, where the receiving antenna was *displaced along a track*. Measurements in the corridor (3.5 m in width) and the adjoining Room II included typical locations G and H, respectively (*with antenna displacement*).

Room I consists of three sections. Section 1 is the main part, with wooden benches, desks, bookcases, and workstation terminals. Soft partitions of glass separate section 1 from section 2 and a reinforced concrete wall separates section 2 from section 3. The walls of Room I are made of brick and stone covered with plaster and the dimensions are 6.8 m length, 8 m width, and 3.5 m height. There are three glass windows, in large wooden frames, 2 m long and 2.5 m high, which were closed during the measurement process.

The dimensions of Room II are 15 m length, 5 m width, and 3.5 m height. Room II is a typical laboratory with six series of benches and three glass windows with the same dimensions as those in Room I. Several positions were selected such as to include LOS, NLOS, and obstructed topographies representing typical conditions within a building. Measurements at position E in Room I were conducted in the presence of a reflector (1 m^2) in order to examine changes in the environment caused by a perfectly conducting known surface. Transmitter–receiver antenna separations were 5.5 m for locations A and E, 6 m for location B, 4.3 m for location C, 2.8 m for location D, 3.7 m for position F, 16.4 m for position G, and 13.2 m for position H.

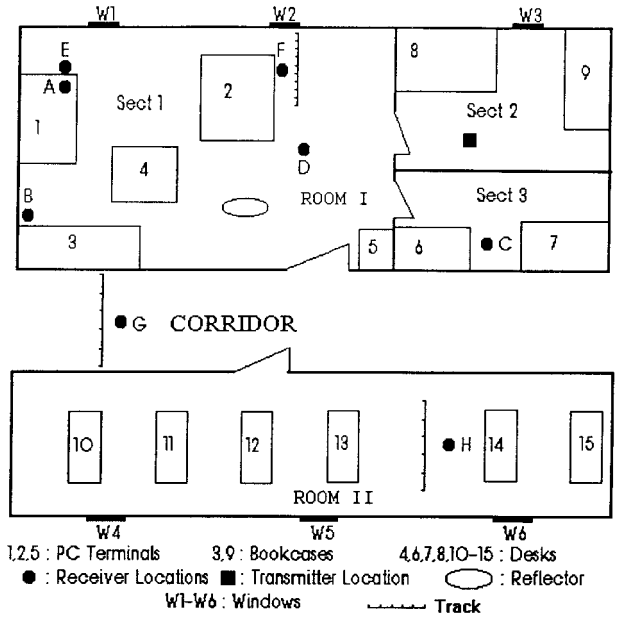

Fig. 1. Plan of the measured indoor environment with transmitter and receiver antenna location.

The measurement scenario in locations F, G, and H involved consecutive measurements at selected positions of the receiving antenna along a 1.5-m track. For each of the measured positions, 30 impulse response profiles of the channel were recorded. Then by consecutively displacing the portable antenna from one position to the other, the whole track length was covered. By following the above technique, we assume that the channel's characteristics do not significantly change over short tracks, and therefore changes in statistics can be considered as local variations [2]. The scenario is illustrated in Fig. 1 (locations F, G, and H). During the measurement process in location H, people were moving inside Room II (*case H personnel movement*).

3. MEASUREMENT SETUP

The measurement setup is shown in Fig. 2. The system consists of a synthesized sweeper and an HP 8510 B network analyzer. A signal generated by the synthesized source is transmitted and the received signal is detected. In this method the channel is excited with tones over a wide frequency range. Magnitude and phase shift of each frequency component are recorded.

The output of the network analyzer (port 1 of the S-parameter device) was connected to a wideband amplifier with maximum output level of 35 dBm through a 5-m coaxial cable. Due to the attenuation of the coaxial cable connected between the transmitting antenna and port 1, the actual transmitting power is 30 dBm. The receiving antenna was connected directly to port 2 of the S-parameter device through a 25-m coaxial cable. The transmitting antenna height was maintained constant at 1.8 m. The receiving antenna height was 1.75 m for all measured sites. All measurement tests involved transmitting and receiving omnidirectional, vertically polarized $\lambda/4$ antennas, with 2.1 dBi gain, chosen for their wide bandwidth.

The measurement system is controlled by a PC via an HPIB interface. Measurement data were downloaded to the computer for further analysis. Before the measurements were carried out, the system was calibrated at the frequency band of interest in order to compensate for the influence of phase and amplitude variations imposed by cables and amplifier.

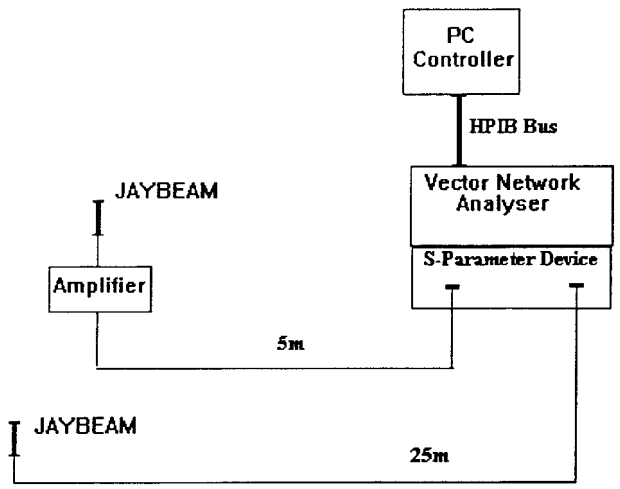

Fig. 2. Block diagram of the indoor measurement setup.

4. MEASUREMENTS RESULTS

The measured parameter is the S_{21}. The signal arriving at port 2 of the network analyzer is measured with respect to the one transmitted from port 1. The S_{21} parameter is the ratio of the received to the transmitted voltage as a function of frequency [3, 9]. The network analyzer is capable of taking a maximum of 801 frequency points per sweep. In this way the frequency response of the propagation channel is obtained by recording the amplitude and phase of the received to the transmitted signal. The recording time was approximately 1.5 s for each measured impulse response profile. Magnitude and phase profiles are presented in Figs. 3 and 4. A reasonable assumption for the ray phases is that they are mutually independent random variables which are uniformly distributed over $[-\pi, \pi]$ due to the fact that the ray phase is subject to alteration as the path length changes. This consideration was verified for all measurement data sets. Measurement data were windowed by using a Kaiser Window technique [11] and zero padded to the next highest number, 1024 (which is a power of two). The time domain of the channel response is obtained from the measured data using the inverse FFT. For all measurements care was taken to select an appropriate time span large enough to capture all significant power delay paths. The measurement bandwidth

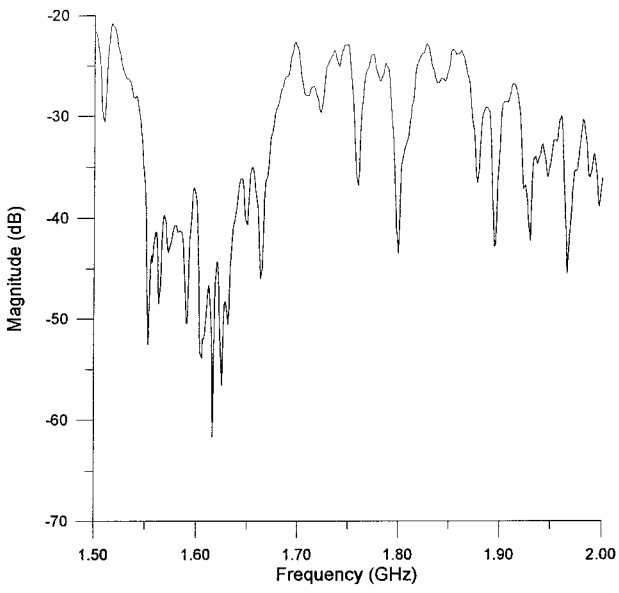

Fig. 3. Magnitude (dB) profile of a typical measured frequency response.

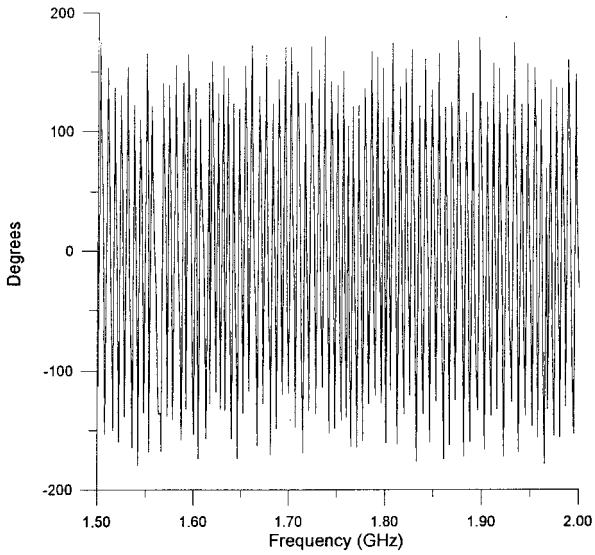

Fig. 4. Phase profile of a typical measured frequency response.

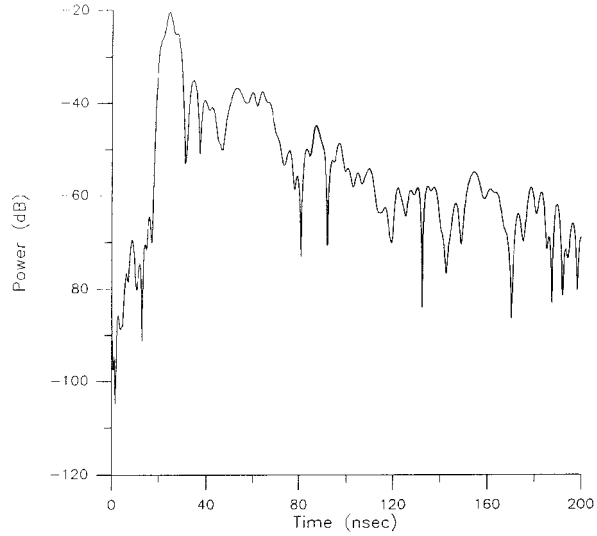

Fig. 5. Mean power delay profile for LOS location A.

was taken as 0.5 GHz, which results in an equivalent time domain resolution of 2 ns.

Five sets of static measurements were conducted in Room I with the receiving antenna placed at a different places for each set of measurements. During the measurement process inside Room I there was no personnel present, so the channel can be considered as static. The measurement scheme inside Room I can be divided into the following cases: those where LOS existed between transmitter and receiver (locations A, B, and D), and the NLOS case, where a brick and stone wall separated the transmitting from the receiving antenna (location C).

To obtain the average power delay profile (PDP), each individual power delay profile is weighted by its normalized received power value. Average impulse response profiles for the LOS case (location A) is shown in Fig. 5, whereas Fig. 6 illustrates the average impulse response profile for the NLOS case (location C).

A measurement test was also conducted with (location A) and without (location E) the presence of a reflector made of aluminum located in the middle of section 1, as shown in Fig. 1, in order to examine the effect of reflection from a known surface. The impulse response profile for the reflector case is shown in Fig. 7. More reflected signals can easily be distinguished due to the presence of the reflecting surface. Strong signals between 50 and 150 ns are present due to the reflector surface positioned 4 m from the transmitting antenna. The average level of the multipath components which arrived within the above range are about 8 dB larger than those that occurred in the same location without the reflector (A).

The main component in the NLOS case (location C, Fig. 6) is about 15 dB weaker than that in A. For NLOS case measurements tests were made for two different receiving antenna locations in section 3 (one close to desk 6 and one close to the partition between section 2 and section 3), with no significant changes in the main component.

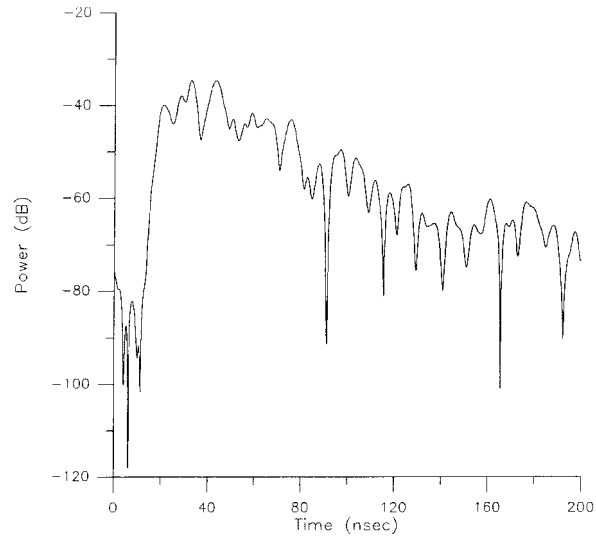

Fig. 6. Mean power delay profile for NLOS location C.

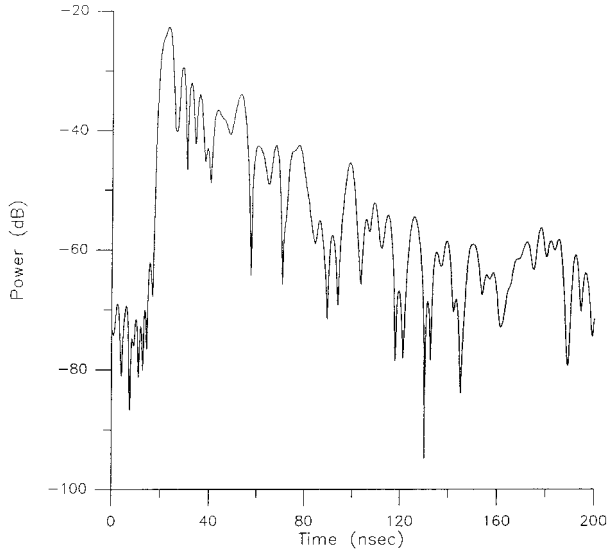

Fig. 7. Mean power delay profile for location E (reflector).

Figure 8 illustrates a typical spatial fluctuation with the receiver moved along the 1.5-m track at location G.

4.1. Consideration and Statistical Modeling of Amplitude and rms Delay Spread

To determine which distribution is the best approximation to describe the amplitude fading variation, the MSE (minimum square error) test was employed between experimental and theoretical distributions normally encountered in a typical indoor radio environment (i.e., Rice, Rayleigh). The parameters involved in the theoretical distribution functions were estimated by using the moment methods in which the first and second moments of the theoretical distributions are equated with the corresponding empirical ones calculated from the measured data. The smallest MSE indicates the best distribution function. Table I summarizes the results for the LOS and NLOS cases. Measured data collected from LOS and NLOS sites were tested with both Rician and Rayleigh distributions. The Rician distribution was found to describe the LOS data sets, whereas NLOS data sets follow a Rayleigh distribution as shown in Figs. 9 and 10.

Table I. Mean Square Error Between Theoretical and Experimental Distributions for Amplitude Fading

Location	MSE-Rayleigh	MSE-Rician
F (LOS)	0.87	0.61
G (NLOS)	1.11	3.01
H (NLOS)	1.52	2.04

The entire pool of data collected in the indoor environment indicates that the rms delay spread is slightly smaller than 35 ns and has an approximately normal distribution, as shown in Fig. 11.

Table II shows the values for τ_{rms} delay spread parameter for three configurations (LOS, NLOS, and with the reflector). It can be seen that τ_{rms} is less in locations A, B, and D than in the NLOS case (location C). The smallest rms value is observed in the location A, where Tx–Rx separation is 5 m. The rms delay spread

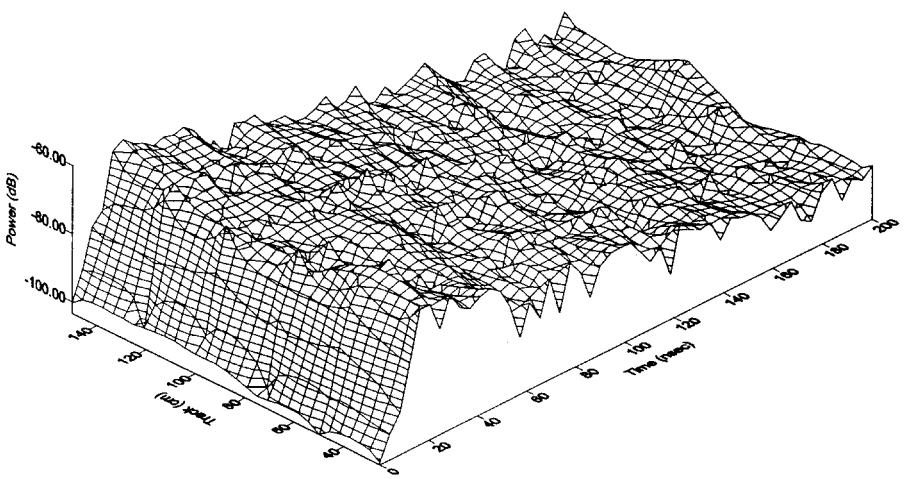

Fig. 8. Typical spatial fluctuations of power IR with the receiver moved along a 1.5-m track in NLOS topography (location G).

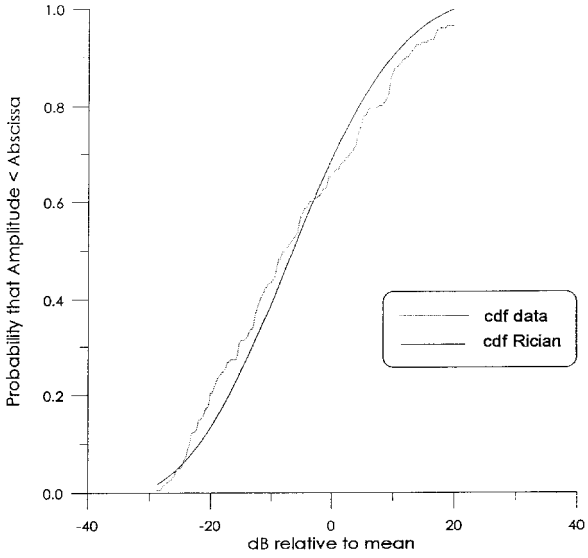

Fig. 9. Comparison between theoretical and experimental amplitude distributions for LOS (location F).

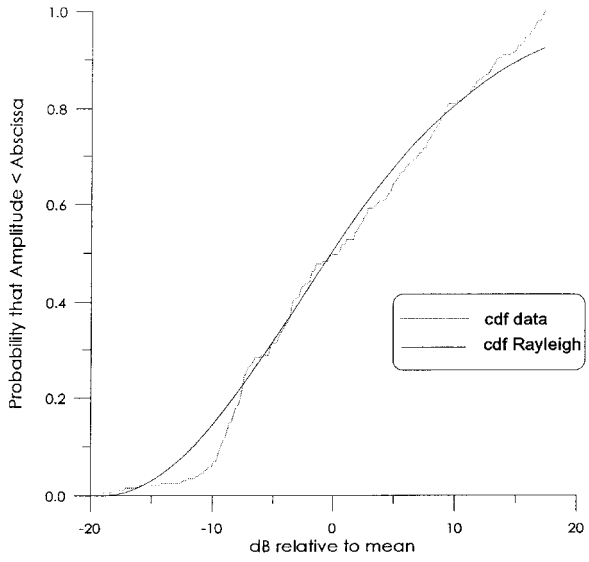

Fig. 10. Comparison between theoretical and experimental amplitude distributions for NLOS (location G).

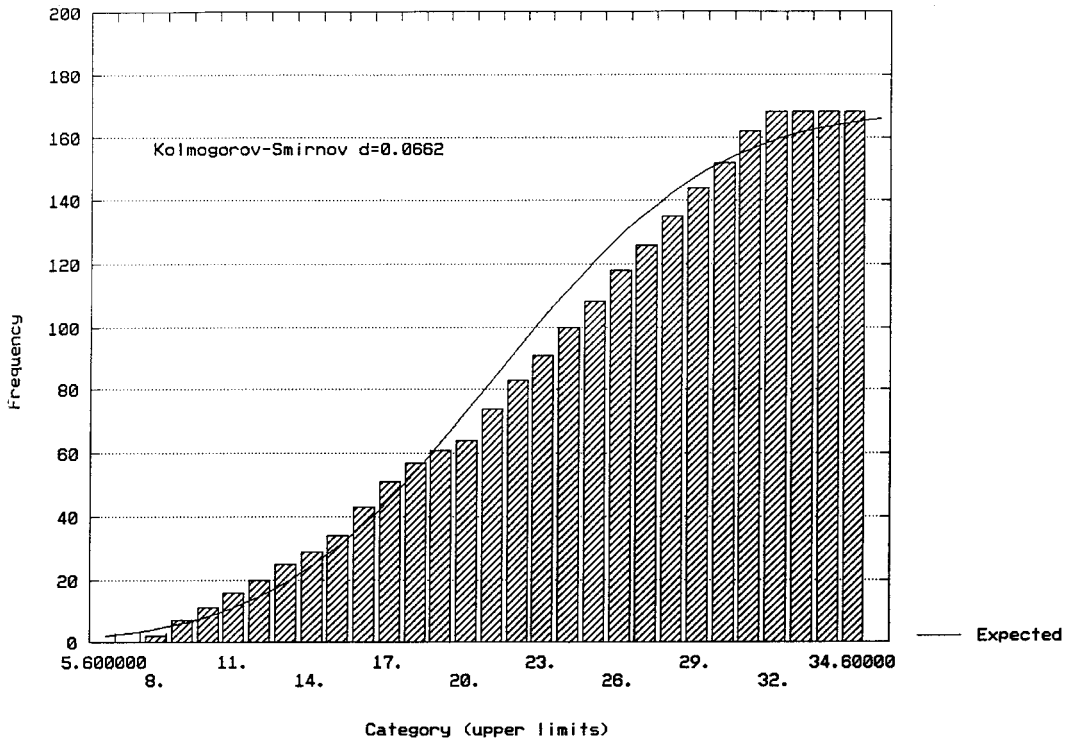

Fig. 11. Expected (normal) and measured cumulative distributions of overall τ_{rms} values.

Table II. The rms Delay Spread for Locations A, B, C, D, and E (Receiving Antenna Static)

Location	Configuration	τ_{rms} (ns)
A	LOS	8.7
B	LOS	15.2
C	NLOS	24.5
D	LOS	17.5
E	Reflector	12.5

values in section 1 vary between 8.7 and 17.5 ns; however, it was observed that the rms delay spread remains fairly constant throughout section 3 (24.5 ns).

Tables III–V illustrates τ_m and τ_{rms} values for positions F–H, respectively. These values were estimated from the 30 consecutive impulse response profiles collected in each one of the selected measured positions as described previously. Table VI shows the mean, maximum, minimum, and standard deviation for locations F–H.

Examination of Table VI shows that the standard deviation of τ_{rms} is greater in location H (Room II), where the signal is obstructed by various surrounding obstacles (metal doors, desks, walls), compared to location F (Room I), where the number of reflections is less. Mean and standard deviation of global rms delay spread values at specific positions were calculating by including the multipath components with amplitudes within 10, 20, or 30 dB of the peak value of the profile.

Table III. Mean τ_m and τ_{rms} Values at Each Measured Position for Location F (Room I) Along a Track of 1.5 m (Receiving Antenna Displacement)

Position	τ_m (ns)	τ_{rms} (ns)
F1	25.7	15.6
F2	16.4	9.1
F3	16.9	8.8
F4	15.3	7.8
F5	20.1	10.7
F6	16.2	9.2
F7	17.3	10.6
F8	29.7	16.1
F9	19.3	12.7

Table IV. Mean τ_m and τ_{rms} Values at Each Measured Position for Location G (Corridor) Along a Track of 1.5 m (Receiving Antenna Displacement)

Position	τ_m (ns)	τ_{rms} (ns)
G1	39.1	29.4
G2	35.1	26.3
G3	40.6	28.7
G4	41.8	27.3
G5	36.1	23.6
G6	33.4	21.3

Table V. Mean τ_m and τ_{rms} Values at Each Measured Position for Location H (Room II) Along a Track of 1.5 m (Receiving Antenna Displacement)

Position	τ_m (ns)	τ_{rms} (ns)
H1	33.2	20.8
H2	36.7	22.7
H3	34.9	21.6
H4	34.7	24.6
H5	44.6	30.4
H6	20.1	16

Table VI. Mean, Standard Deviation, Maximum, and Minimum of rms Delay Spread for All Positions at Locations F, G, and H and Threshold Levels of 10, 20, and 30 dB

Threshold level (dB)	Location	Mean (ns)	Standard deviation	Maximum (ns)	Minimum (ns)
10	F (LOS)	11.2	2.8	17.5	7.7
	G (NLOS)	26.1	3.1	32.5	20.1
	H (NLOS)	22.7	4.4	33.1	15.1
20	F (LOS)	12.5	2.5	18.9	8.2
	G (NLOS)	26	5	35.4	19.5
	H (NLOS)	25.5	4.8	31.6	16.3
30	F (LOS)	15.6	2.9	19.5	10.5
	G (NLOS)	27.4	4.2	34.8	21.6
	H (NLOS)	30.6	5.1	38.6	22.5

During the measurement process at location H at positions H1, H2, H3, and H4 the τ_{rms} values did not greatly vary, although the motion of people influences the τ_{rms} values when moving from position H4 to H5 and H6.

For the statistical analysis of rms delay spread a Kolmogorov–Smyrnov test was employed [4]. The Kolmogorov statistical parameter d is the largest absolute difference between the cumulative observed and expected distributions. As can be observed from the experimental and theoretical distributions in Figs. 12 and 13, τ_{rms} values for NLOS locations can be very well approximated with a normal distribution.

4.2. Simulation Test Results Using SIRCIM

Measured impulse response data were compared with simulation results extracted from SIRCIM [5]. SIRCIM is an indoor UHF multipath radio channel software simulator designed from over 50,000 wideband and narrowband measurements from many different buildings. An omnidirectional, vertically polarized antenna with a 1.8 dBi gain is used for both transmitter and receiver units. The receiver was placed at several locations throughout different open-plan buildings. At each location the receiver was moved along a straight path that was 4.5λ long, that is, 1 m at 1300 MHz. Each location has an associated transmitter–receiver separation distance and is classified by one of two surrounding topographies. The original measurements were carried out at 1300 MHz, but the program was extended to simulate radio channel up to 60 GHz.

Along each 4.5λ track, multipath power delay profiles were recorded with a 7.8-ns probing pulse at 19 discrete locations separated by $\lambda/4$ spacing, thus providing a high enough spatial sample rate to ensure perfect replication of the fading characteristics of individual multipath components as a mobile moves over space. The core of the wideband simulator, which is based on statistical models of all measurements, recreates power delay profiles at $\lambda/4$ separations along simulated 4.5λ tracks with various Tx–Rx antenna separations located throughout different open-plan buildings. SIRCIM produces the statistics of measured wideband impulse responses in both LOS and NLOS topographies and generates 19 baseband complex impulse responses for indoor mobile

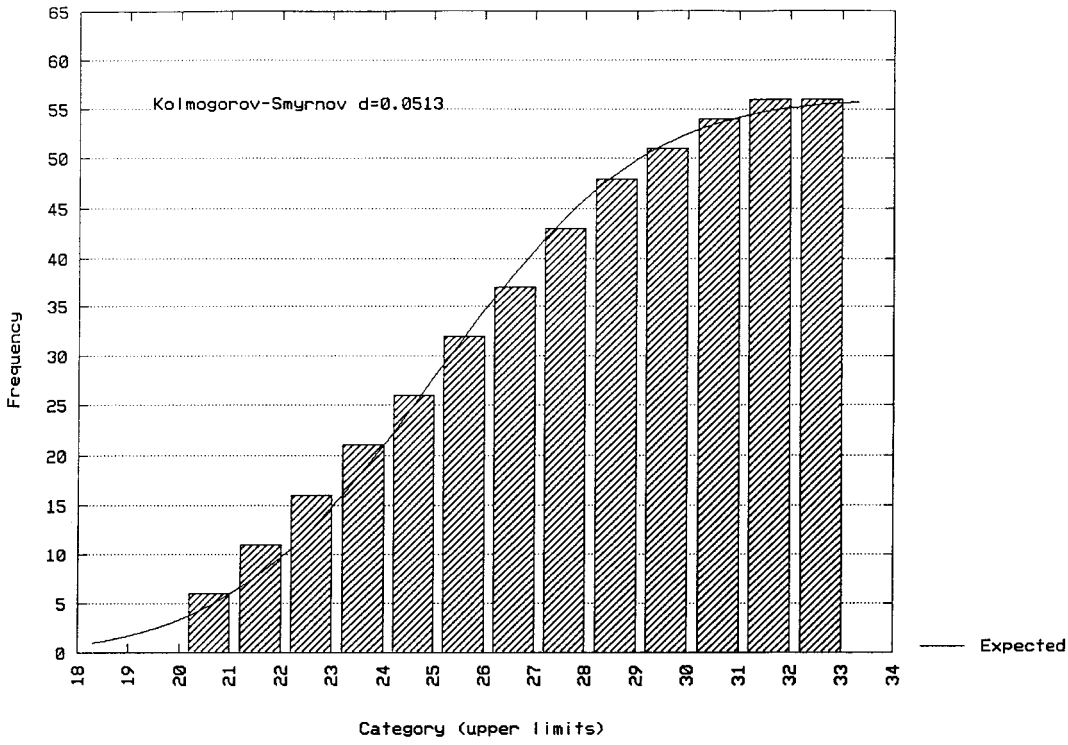

Fig. 12. Expected (normal) and measured cumulative distributions of τ_{rms} values at location G.

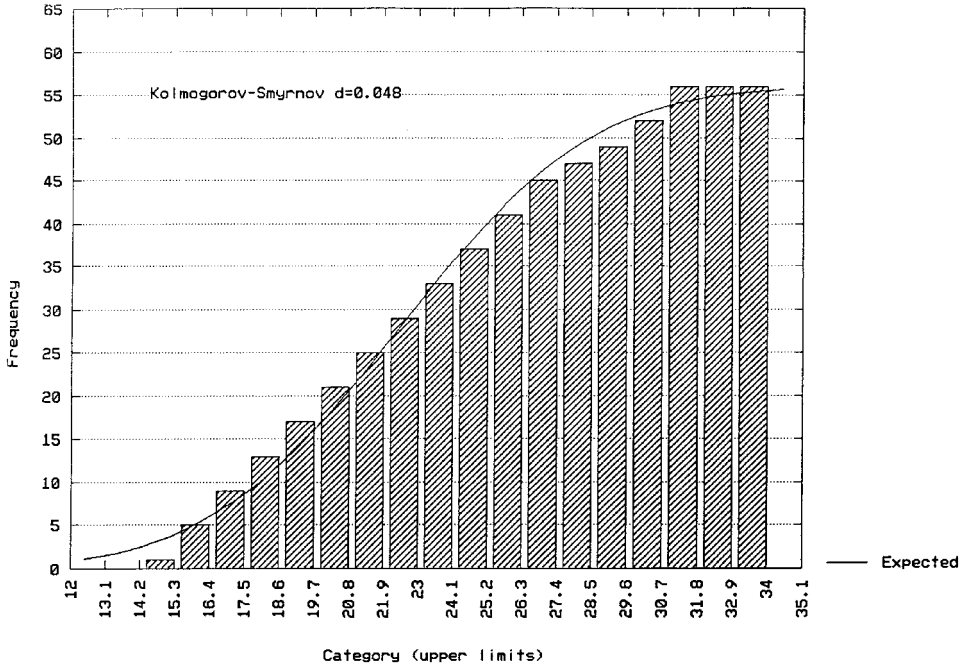

Fig. 13. Expected (normal) and measured cumulative distributions of τ_{rms} values at location H.

radio channels when traveling over a small area (track). Each multipath impulse response is simulated over an excess delay range of 500 ns. The wideband impulse responses are depicted in a linear relative power for excess delays of 0–500 ns.

Figures 14–16 compare measured and simulated data for locations F–H, respectively. We can observe a good approximation for both LOS and NLOS cases, indicating the effectiveness of the SIRCIM Simulator in this particular indoor environment.

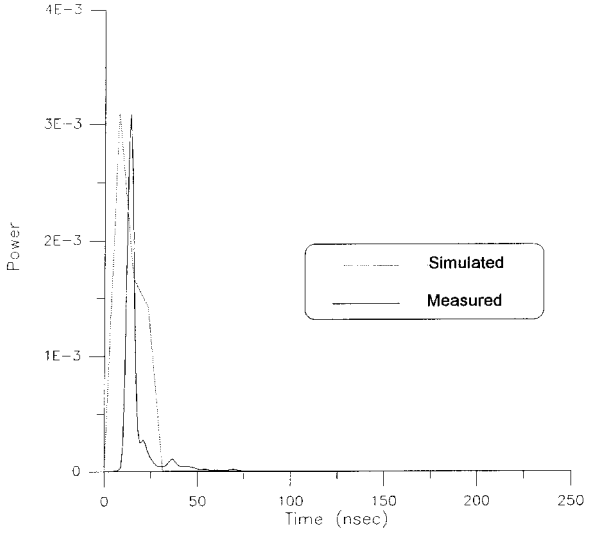

Fig. 14. Comparison of simulated and measured data at location F.

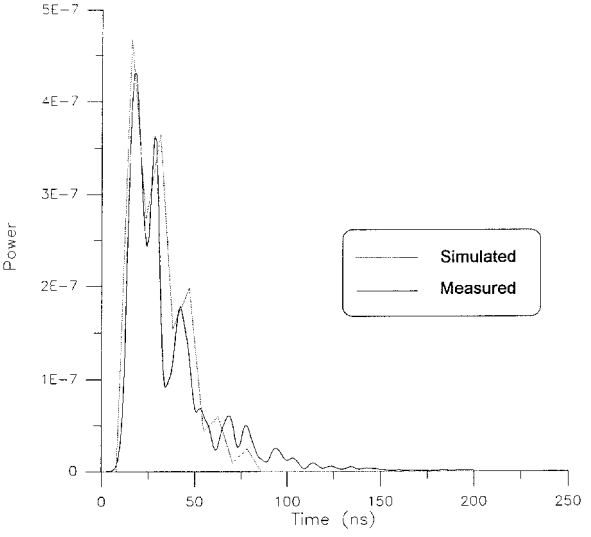

Fig. 15. Comparison of simulated and measured data at location G.

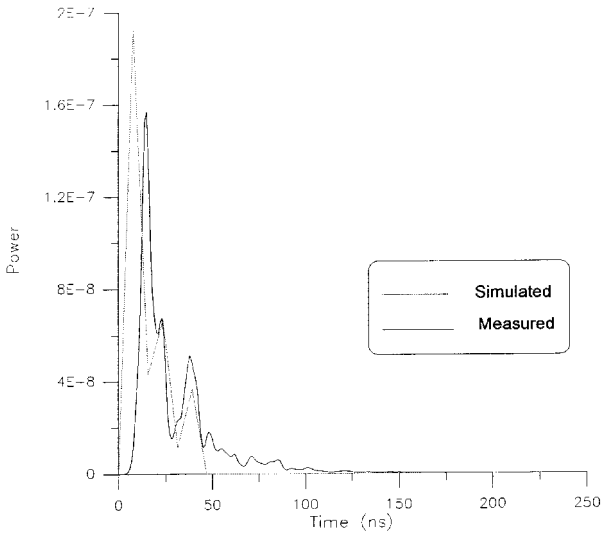

Fig. 16. Comparison of simulated and measured data at location H.

5. CONCLUSIONS

This paper has presented the results of impulse response measurements in an indoor radio channel. In order to characterize the indoor radio channel, measurements were performed at 1.8 GHz. The core of the measurement apparatus is a network analyzer which provides both amplitude and phase domain characteristics. The inverse fast Fourier transform was used to convert the frequency domain data to alternative time domain responses. Typical measured profiles have been collected in different configurations of an indoor environment.

From the measurements results the following points can be summarized:

1. The mean rms values are in general greater in NLOS cases, where the direct path between transmitter and receiver is not clear, as compared to LOS cases.
2. Standard deviation of the rms values seems to correlate with the surrounding environment between transmitter and receiver.
3. The mean rms values estimated within the examined indoor environment are found not to be strongly dependent upon the transmitter–receiver antennaseparation.
4. The values of mean RMS delay spread are typical of those found in similar indoor environments and were found to adhere to a normal distribution. Amplitude fading follows a Rayleigh distribution for the NLOS case and a Rician distribution for the LOS case.

Simulation tests using the SIRCIM software simulator were performed in order to examine the validity of the program. Repeated comparisons of measured and simulated data were examined for all measurement topologies. Measured data for LOS, NLOS, and OBOS cases were found to closely follow the results extracted from the SIRCIM Simulator.

REFERENCES

1. G. L. Turin, A statistical model of urban multipath propagation, *IEEE Transactions on Vehicular Technology*, Vol. 21, pp. 1–9, February 1972.
2. H. Hashemi and D. Tholl, Statistical modelling and simulation of the RMS delay spread of indoor radio propagation channels, *IEEE Transactions on Vehicular Technology*, Vol. 43, No. 1, February 1994.
3. K. Pahlavan and S. J. Howard, Frequency domain measurements of indoor radio channels, *Electronics Letters*, Vol. 25, pp. 1645–1647, 1989.
4. H. Nikookar and H. Hashemi, Statistical modelling of amplitude fading of indoor radio propagation channels. In *Proceedings of 2nd International Conference on Universal Personal Communications*, Ottawa, Canada, Vol. 1, pp. 84–88, 1993.
5. T. S. Rappaport, S. Y. Seidel, P. M. Koushik, and L. McCulley, SIRCIM: Simulation of Indoor Radio Impulse Response Models, Version 2.0, April 1992.
6. H. Zaghloul, G. Morrison, and M. Fattouche, Frequency response and path loss measurements of indoor channel, *Electronics Letters*, Vol. 27, pp. 1021–1023, 1991.
7. Peter Carlson and Lars Olsson, Time dispersion measurement system for radio propagation at 1800 MHz and results from typical indoorenvironments. In *Proceedings of 44th Vehicular Technology Conference*, Stockholm, Sweden, 1994.
8. T. A. Sexton and K. Pahlavan, Channel modelling and adaptive equalisation of indoor channels, *IEEE Journal on Selected Areas in Communication*, Vol. JSAC-5, pp. 128–137, February 1987.
9. S. Howard and K. Pahlavan, Measurements and analysis of the indoor radio channel in the frequency domain, *IEEE Transactions on Instrumentation and Measurements*, Vol. IM-38, pp. 751–755, October 1990.
10. T. S. Rappaport, Characterisation of UHF multipath radio channels in factory buildings, *IEEE Transactions on Antennas and Propagation*, Vol. 37, No. 8, pp. 1058–1069, August 1989.
11. F. J. Harris, On the use of windows for harmonic analysis with the discrete Fourier transform, *Proceedings of the IEE*, Vol. 66, No. 1, January 1978.

Nikolaos Papadakis received the Diploma in Electrical Engineering from the National Technical University of Athens, Greece, in 1992. He is currently working toward his Ph.D. degree. He has participated in RACE II and COST231 projects. His main fields of interest propagation and channel modeling in indoor and outdoor environments. He is also a member of the Technical Chamber of Greece.

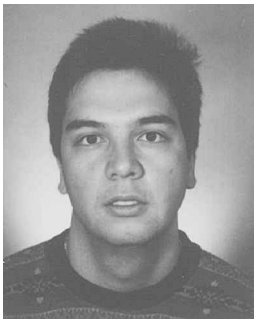

Antonis Hatziefremidis was born in Athens, Greece, in 1972. He received the Diploma in Electrical and Computer Engineering from the National Technical University of Athens in July 1995. His research interests are in the area of wireless and optical communication. He is currently working toward the Ph.D. degree in optical communication at the National Technical University of Athens. He is also member of Optical Society of America and Technical Chamber of Greece.

Anastasios Tserolas was born in Aliveri-Evia, Greece, in 1972. He has received his Diploma in Electrical and Computer Engineering from National Technical University of Athens and he is now involved in the area of wireless personal communications.

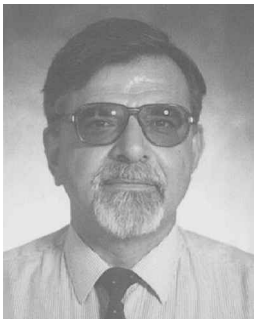

Philip Constantinou received the Diploma in Physics from the National University of Athens in 1972, the Master of Applied Science in electrical engineering from the University of Ottawa, Ontario, Canada, in 1976, and the Ph.D. degree in electrical engineering in 1983 from Carleton University, Ottawa, Ontario, Canada. From 1976 to 1979, he was with Telesat Canada as Communications System Engineer. In 1980, he joined the Ministry of Communications in Ottawa, Canada, where he was engaged in the area of mobile communications. From 1984 to 1989, he was with the National Research Centre Demokritos in Athens, Greece, where he was involved in several research projects in the area of mobile communications. In 1989, he joined the National Technical University of Athens, where he is currently Professor and Director of the Mobile Communications Laboratory. His current research interests include personal communications, mobile satellite communications, and interference problems in digital communications systems.